Inorganic Chemistry

Article

Origin of Compressed Jahn–Teller Octahedra in Sterically Strained Manganese(III) Complexes

Philip L. W. Tregenna-Piggott*

*Laboratory for Neutron Scattering, ETH Zürich and Paul Scherrer Institut,
CH-5232 Villigen PSI, Switzerland*

A method is presented that enables the bond length changes resulting from the Jahn–Teller interaction to be predicted from a knowledge of the angular geometry of the complex and the identity of the ligators. The calculation of the energy minimum within the subspace of the Jahn–Teller active *e* skeletal mode proceeds by diagonalization of the potential energy component of the cubic E⊗*e* Jahn–Teller problem, incorporating low-symmetry distortions by way of angular overlap model calculations. The theory is applied to a series of manganese(III) complexes formed with tetradentate tripodal ligands that largely dictate the angular coordinates. A good account of the contrasting molecular structures is obtained by allowing the σ-bonding strength to vary according to expectations based upon the spectrochemical series.

1. Introduction

The ubiquity of manganese throughout biology is rendered primarily by the rich redox chemistry of the element, with monomeric manganese(III) implicated in a number of biological systems.[1] The cation is both redox-active and possesses a labile coordination sphere on account of the Jahn–Teller effect. Recent attempts to synthesize mimics of manganese(III) active centers have resulted in a series of complexes among which are those that exhibit a tetragonally compressed geometry.[2] From the perspective of an inorganic chemist whose preoccupation is the manifestation of the Jahn–Teller effect in coordination compounds,[3–10] this result is rather striking, as a tetragonally compressed manganese-

(III) octahedron is rare indeed, which may be realized only under very particular circumstances. While we are not aware of a biological system where it has been proven that the activity is linked to a compressed rather than an elongated octahedron, the dynamics of the coordination sphere changes continually as a compressed octahedron becomes more competitive with the elongated counterpart. It is necessary, therefore, to identify the factors that favor a tetragonally compressed geometry in these manganese(III) compounds. It is this problem with which we shall be concerned.

The common occurrence of axially elongated octahedra in d^9 and high-spin d^4 complexes in coordination compounds is commonly attributed to the additional stabilization of the $3d_{z^2}$ orbital via interaction with the 4s orbital and anharmonic contributions to the vibrational potential.[11–13] Compressed octahedra are, however, clearly competitive in complexes where the angular distortion of the first coordination sphere imposed by a polydentate ligand is great.[2,14,15] The current

* To whom correspondence should be addressed. E-mail: philip.tregenna@psi.ch.

(1) Weatherburn, D. C. Manganese-containing enzymes and proteins. In *Handbook on Metalloproteins*; Bertini, I.; Sigel, A.; Sigel, H., Eds.; New York: Marcel Dekker, 2001, 193−268. Siegbahn, P. E. M. *Curr. Opin. Chem. Biol.* **2002**, *6*, 227.

(2) Triller, M. U.; Pursche, D.; Hsieh, W.; Pecoraro, V. L.; Rompel, A.; Krebs, B. *Inorg. Chem.* **2003**, *42*, 6274.

(3) Dobe, C.; Noble, C.; Carver, G.; Tregenna-Piggott, P. L. W.; McIntyre, G. J.; Barra, A.-L.; Neels, A.; Janssen, S.; Juranyi, F. *J. Am. Chem. Soc.* **2004**, *126*, 16639.

(4) Tregenna-Piggott, P. L. W.; Weihe, H.; Barra, A.-L. *Inorg. Chem.* **2003**, *42*, 8504.

(5) Krivokapic, I.; Noble, C.; Klitgaard, S.; Tregenna-Piggott, P. L. W.; Weihe, H.; Barra, A.-L. *Angew. Chem.* **2005**, *44*, 3613.

(6) Carver, G.; Spichiger, D.; Tregenna-Piggott, P. L. W. *J. Chem. Phys.* **2005**, *122*, 124511.

(7) Tregenna-Piggott, P. L. W.; Carver, G. *Inorg. Chem.* **2004**, *43*, 8061.

(8) Tregenna-Piggott, P. L. W.; Andres, H-P.; McIntyre, G. J.; Cowan, J. A.; Best, S. P.; Wilson, C. C. *Inorg. Chem.* **2003**, *42*, 1350.

(9) Dolder, S.; Spichiger, D.; Tregenna-Piggott, P. L. W. *Inorg. Chem.* **2003**, *42*, 1343.

(10) Basler, R.; Tregenna-Piggott, P. L. W.; Andres, H.; Dobe, C.; Gudel, H.; Janssen, S.; McIntyre, G. J. *J. Am. Chem. Soc.* **2001**, *123*, 3377.

(11) Riley, M. J. *Top. Curr. Chem.* **2001**, *214*, 5.

(12) Deeth, R. J.; Hitchman, M. A. *Inorg. Chem.* **1986**, *25*, 1225.

(13) Figgis, B. N.; Hitchman, M. A. *Ligand-Field Theory and Its Applications*; Wiley-VCH: New York, 2000.

(14) Mantel, C.; Hassan, A. K.; Pecaut, J.; Deronzier, A.; Collomb, M. N.; Duboc-Toia, C. *J. Am. Chem. Soc.* **2003**, *125*, 12337.

(15) Holland, J. M.; Liu, X.; Zhao, J. P.; Mabbs, F. E.; Kilner, C. A.; Thornton-Pett, M.; Halcrow, M. A. *J. Chem. Soc., Dalton Trans.* **2000**, 3316.

1.

2.

3.
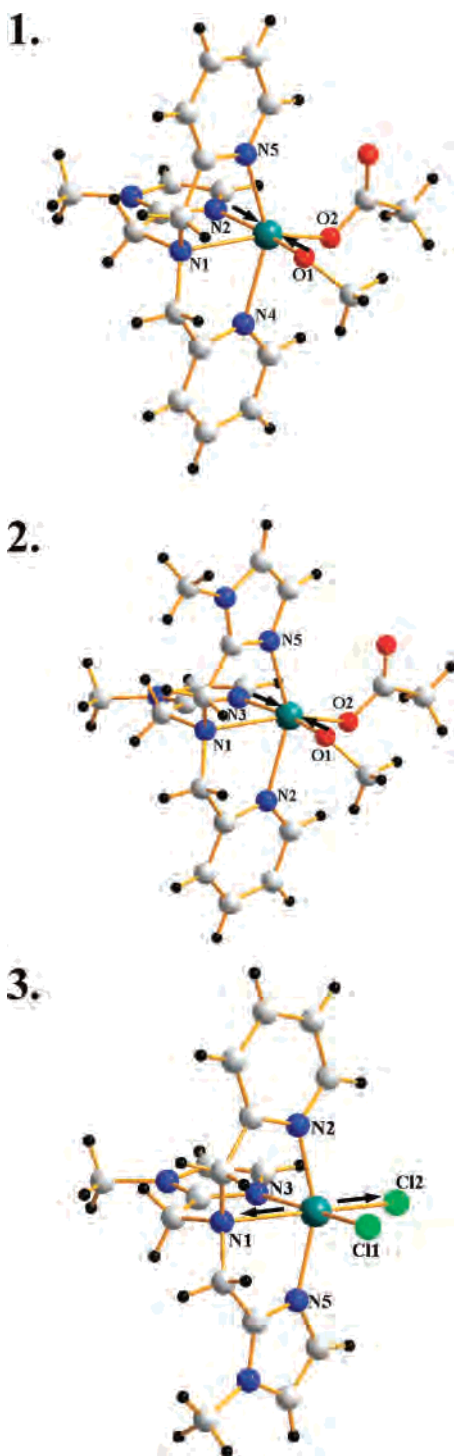
Figure 1. Structure of **1**−**3**. The unique short (**1** and **2**) or long (**3**) axes are indicated by means of arrows.

fashion for addressing why this is so is to perform a computationally intense calculation, under an acronym that few would comprehend,[16] to show that the experimental structures do indeed correspond to the optimized geometries. Though electronic structure calculations have been employed successfully on Jahn−Teller active homoleptic complexes

Table 1. Manganese(III)−Ligand Bond Distances[2] for Complexes **1**−**3**

Mn−ligand bond lengths/Å	complex **1**	complex **2**	complex **3**
Mn−O(1)	1.777(3)	1.820(3)	
Mn−O(2)	1.955(3)	1.969(3)	
Mn−O(3)			
Mn−N(1)	2.286(3)	2.330(3)	2.365(3)
Mn−N(2)	2.014(3)	2.225(3)	2.069(3)
Mn−N(4)	2.243(3)		
Mn−N(3)		2.024(3)	2.007(3)
Mn−N(5)	2.218(3)	2.163(3)	2.042(3)
Mn−Cl(1)			2.224(1)
Mn−Cl(2)			2.362(1)

to extract coupling constants,[17−19] the location of the global minimum in large low-symmetry complexes is, as we have found,[20] not straightforward. In this paper, we demonstrate that the underlying reason why an axially compressed octahedral geometry is competitive in these bioinorganic manganese(III) complexes can be appreciated by considering how the angular strain imposed by an asymmetric ligand field perturbs a cubic E⊗e Jahn−Teller potential energy surface. This approach is certainly crude given the large deviation from cubic symmetry in the systems we shall be considering. Nevertheless, an all-important intuitive feel for the factors governing the stereochemistry of the complex is obtained.

The compounds chosen for analysis are [Mn(bpia)(OAc)-(OCH$_3$)](PF$_6$) (**1**), [Mn(bipa)(OAc)(OCH$_3$)](PF$_6$) (**2**), and [Mn(bipa)Cl$_2$](ClO$_4$) (**3**), depicted in Figure 1, where bpia and bipa are the tripodal ligands bis(picolyl)(*N*-methylimidazole-2-yl)amine and bis(*N*-methylimidazole-2-yl)(picolyl)-amine, respectively. The manganese(III)−ligand bond lengths are documented in Table 1. Compounds **1** and **2** exhibit a compression along the N(2)−Mn(1)−O(1) and N(3)−Mn-(1)−O(1) axes, respectively, whereas **3** exhibits an elongation along the Cl(2)−Mn(1)−N(1) axis. These structural features are fully consistent with theoretical predictions, where the primary input is the relative σ-bonding strengths of the coordinating ligands.

2. Theory

The Hamiltonian is written as

$$\hat{H} = \hat{H}_{cub} + \hat{H}_{ph} + \hat{H}_{JT} + \hat{H}_{st} \tag{1}$$

$\hat{H}_{cub}$ designates the cubic component of the ligand field that results in the doubly degenerate ground term. The energy of the orbital doublet is set to zero for convenience. $\hat{H}_{ph}$, the Hamiltonian for an e$_g$ phonon mode before coupling, can be written as[21]

$$\hat{H}_{ph} = [0.5\hbar\omega(\hat{P}_\theta^2 + \hat{P}_\epsilon^2 + \hat{Q}_\theta^2 + \hat{Q}_\epsilon^2)]\hat{U}_\tau \tag{2}$$

where $\hbar\omega$ is the phonon energy and $\hat{P}_i$ and $\hat{Q}_i$ are dimensionless operators representing the momenta and distortion

(16) Scheifele, Q.; Riplinger, C.; Neese, F.; Weihe, H.; Barra, A.-L.; Juranyi, F.; Podlesnyak, A.; Tregenna-Piggott, P. L. W. *Inorg. Chem.* **2008**, *47*, 439−447.

(17) Bruyndonckx, R.; Daul, C.; Manoharan, P. T.; Deiss, E. *Inorg. Chem.* **1997**, *36*, 4251.

(18) Atanasov, M.; Comba, P.; Daul, C. A.; Hauser, A. *J. Phys. Chem. A* **2007**, *111*, 9145−9163.

(19) Reinen, D.; Atanasov, M.; Massa, W. *Z. Anorg. Allg. Chem.* **2006**, *632*, 1375.

(20) Neese, F.; Tregenna-Piggott, P. L. W., work in progress.

(21) Tregenna-Piggott, P. L. W. *Adv. Quantum Chem.* **2003**, *44*, 461.

coordinates. Anharmonic terms have been neglected. To second order, $\hat{H}_{JT}$ has the form[21]

$$\hat{H}_{JT} = A_1(\hat{Q}_\theta\hat{U}_\theta + \hat{Q}_\epsilon\hat{U}_\epsilon) +$$
$$A_2((\hat{Q}_\epsilon^2 - \hat{Q}_\theta^2)\hat{U}_\theta + 2\hat{Q}_\theta\hat{Q}_\epsilon\hat{U}_\epsilon) \quad (3)$$

where A_1 and A_2 are the first- and second-order Jahn−Teller coupling constants.

The distortion in the $\{Q_\theta,Q_\epsilon\}$ coordinate space is conveniently represented in polar coordinates:

$$Q_\theta = \rho\cos\phi_\rho$$
$$Q_\epsilon = \rho\sin\phi_\rho \quad (4)$$

$\hat{U}_\theta$, $\hat{U}_\epsilon$, and $\hat{U}_\tau$ are electronic operators, active in the θ, ϵ orbital basis of the ^5E_g ground term of the manganese(III) complex:

$$\hat{U}_\tau = \begin{pmatrix} 1 & 0 \\ 0 & 1 \end{pmatrix}, \hat{U}_\theta = \begin{pmatrix} -1 & 0 \\ 0 & 1 \end{pmatrix}, \hat{U}_\epsilon = \begin{pmatrix} 0 & 1 \\ 1 & 0 \end{pmatrix} \quad (5)$$

The strain term H_{st} represents the low-symmetry ligand field and may be written as

$$\hat{H}_{st} = -e_\theta\hat{U}_\theta - e_\epsilon\hat{U}_\epsilon \quad (6)$$

For the ensuing discussion it is also useful to describe the strain in polar coordinates. By analogy with eq 4 we write

$$e_\theta = \delta\cos\phi_\delta$$
$$e_\epsilon = \delta\sin\phi_\delta \quad (7)$$

The signs of the parameters comprising the Hamiltonian are defined such that the effect of strain alone will be to localize the minimum at the value $\phi_\rho = \phi_\delta$, while the cubic Jahn−Teller interaction results in minima at $\phi_\rho = 0°$, 120°, and 240°. The value of ϕ_ρ where the potential energy minimum is located then largely depends on the value of δ relative to the barrier height given by $2\beta \sim 2A_2(A_1/\hbar\omega)^2$. The values for A_1 and $\hbar\omega$ are estimated from optical[4] and Raman[22] spectra of aqua ions. The value for the parameter A_2 is much harder to estimate. It is an effective parameter absorbing the effects of both quadratic coupling and anharmonicity. For the copper(II) hexa-aqua ion, A_2 has been estimated to be $\sim$33 cm^{-1} from modeling of the temperature dependence of spectroscopic and crystallographic data.[23] For copper(II)-doped CaO, the quadratic coupling constant is much smaller, of the order of -1.0 cm^{-1}, as demonstrated by analysis of the electronic Raman spectrum.[21] We are not aware of any experimental measure of A_2 in a manganese-(III) coordination compound. In this work, A_2 is assigned a value of 10 cm^{-1}. The potential energy minimum is then largely dictated by the strain, but the effect of the two competing contributions to the minimum value of ϕ_ρ can still be seen. The positive sign ensures that the natural

tendency of the Jahn−Teller interaction is to stabilize a tetragonally elongated structure.

The strain may be regarded as having two principal contributions. The first is the geometrical distortion arising primarily from the steric constraints imposed by the polydentate ligand. The second is an electronic factor arising from the differing σ-bonding capabilities of the ligands. The effect of lattice forces, which make a significant contribution to the geometry and σ-bonding capabilities of homoleptic complexes,[3,24] is not considered here. Equation 6 should not incorporate the effect of the bond length changes due to the Jahn−Teller effect, as this is already included in eq 3. In a previous study of Cu^{2+}-doped NH$_4$Cl, temperature-dependent g values were modeled using a dynamic Jahn−Teller coupling model and the strain values extracted shown to correlate with the σ-bonding power of the ligands.[25] In this work, the opposite approach is taken. In the framework of the angular overlap model (AOM), the strain may be written in terms of the angular coordinates and σ-bonding strengths of the ligands. Neglecting π-bonding, $\hat{H}_{st}$ has the explicit form

$$\hat{H}_{st} =$$
$$\begin{pmatrix} \sum_i e_\sigma^i[F_\sigma^i(d_{x^2-y^2})]^2 & \sum_i e_\sigma^i[F_\sigma^i(d_{x^2-y^2})][F_\sigma^i(d_{z^2})] \\ \sum_i e_\sigma^i[F_\sigma^i(d_{x^2-y^2})][F_\sigma^i(d_{z^2})] & \sum_i e_\sigma^i[F_\sigma^i(d_{z^2})]^2 \end{pmatrix} \quad (8)$$

where the sum is over all the ligands of the complex, whose positions are described by the polar angles θ and ϕ. The angular overlap factors for the one-electron orbitals are[13]

$$F_\sigma(d_{x^2-y^2}) = \left(\frac{\sqrt{3}}{4}\right)\cos 2\phi(1 - \cos 2\theta)$$

$$F_\sigma(d_{z^2}) = \frac{(1 + 3\cos 2\theta)}{4} \quad (9)$$

The Hamiltonian for the potential energy is then obtained by collecting all the terms in eqs 1−9, ignoring the kinetic energy in eq 2, resulting in the expression given in eq 10.

In the next section we will use eq 10 as follows: The parameters A_1, A_2, and $\hbar\omega$ are fixed at values of -1400, 10, and 450 cm^{-1}, respectively. Different complexes appear in the model by having different $\hat{H}_{st}$ matrix elements. The matrix eq 10 shall be numerically diagonalized, and the surface shall be comprised of the lower eigenvalue plotted as a function of Q_θ and Q_ϵ.

The vibronic eigenvalues of the $^5E{\otimes}e$ Hamiltonian are found according to a numerical method outlined previously.[3] The splitting of the ground S = 2 multiplet may be well described by the conventional second-order spin-Hamiltonian

(22) Best, S. P.; Beattie, J. K.; Armstrong, R. S. *J. Chem. Soc., Dalton Trans.* **1984**, 2611.

(23) Riley, M. J.; Hitchman, M. A.; Mohammed, A. W. *J. Chem. Phys.* **1987**, *87*, 3766.

(24) Masters, V. M.; Riley, M. J.; Hitchman, M. A. *Inorg. Chem.* **2001**, *40*, 843 and references therein.

(25) Riley, M. J.; Hitchman, M. A.; Reinen, D.; Steffen, G. *Inorg. Chem.* **1988**, *27*, 1924.

$$\hat{H}_{\text{P.E.}} =$$

$$\begin{pmatrix} 0.5\hbar\omega(Q_\theta^2 + Q_\epsilon^2) - A_1 Q_\theta - A_2(Q_\epsilon^2 - Q_\theta^2) + \sum_i e_\sigma^i [F_\sigma^i(\text{d}_{x^2-y^2})]^2 & A_1 Q_\epsilon + A_2 2 Q_\theta Q_\epsilon + \sum_i e_\sigma^i [F_\sigma^i(\text{d}_{x^2-y^2})][F_\sigma^i(\text{d}_{z^2})] \\ A_1 Q_\epsilon + A_2 2 Q_\theta Q_\epsilon + \sum_i e_\sigma^i [F_\sigma^i(\text{d}_{x^2-y^2})][F_\sigma^i(\text{d}_{z^2})] & 0.5\hbar\omega(Q_\theta^2 + Q_\epsilon^2) + A_1 Q_\theta + A_2(Q_\epsilon^2 - Q_\theta^2) + \sum_i e_\sigma^i [F_\sigma^i(\text{d}_{z^2})]^2 \end{pmatrix}$$

$$(10)$$

$$\hat{H}_s = D\left[\hat{S}_z^2 - \frac{1}{3}S(S+1)\right] + E[\hat{S}_x^2 - \hat{S}_y^2] \qquad (11)$$

where E and D designate the rhombic and axial zero-field-splitting parameters. The ratio of these parameters is reported for completeness.

The principal assumption in this formulation is that the strain does not break the cubic symmetry of the Hamiltonian. Simply by inspection of the structures in Figure 1 this would seem incredulous. Nevertheless, anticipating the results of the next section, the calculated splitting of the E term due to the strain is ∼3 times less than that produced by the Jahn−Teller interaction and hence may still be broadly considered as a perturbation. Furthermore, given that the aim of this work is to predict where on the Jahn−Teller potential energy surface a complex is distorted, without calculating detailed bond-length changes, the inclusion of further parameters would not be justified.

3. Discussion

In order to gain an appreciation of the influence of the changing ligand field environment on the geometric structure, it is useful to break the Hamiltonian up into its cubic and anisotropic parts. Figure 2 displays a contour plot of a cubic E⊗e Jahn−Teller potential energy surface. With reference to complex **1**, the ligand positions and the sign of the parameters are defined such that $\phi_\rho = 0°/180°$ corresponds to an elongation/compression along the N1−Mn and Mn−O2 bond vectors, $\phi_\rho = 240°/60°$ to an elongation/compression along the N2−Mn and Mn−O1 bond vectors, and $\phi_\rho = 120°/300°$ to an elongation/compression along the N5−Mn and Mn−N4 bond vectors. The minima occur at positions in the potential energy surface corresponding to tetragonal elongations.

In heteroleptic complexes of manganese(III), the ligands tend to arrange themselves so as to provide a tetragonal strain of the same sign, as this is energetically more favorable. For example, in manganese(III) complexes formed with terminal and bridging fluoride ligands, the overwhelming tendency is for a tetragonally elongated geometry with the bridging ligands in the axial positions.[18] The result has been rationalized in terms of the force constant for the Mn(III)−F bond being stronger when the fluoride ligand is terminal rather than bridging.[18] When the coordination positions are largely dictated by polydentate ligands, a compression may become competitive. Overlaid on the cubic E⊗e potential energy surface displayed in Figure 2 are vectors representing the strain interaction calculated using the coordinates of the [Mn-(bpia)(OAc)(OCH$_3$)]$^+$ complex with the e_σ parameters for the nitrogen ligators of the tripodal ligand fixed at 7000 cm^{-1}. The e_σ values for the two remaining ligators are varied

between 4000 and 7000 cm^{-1}, as indicated in the figure. It is seen that the angular coordinate of the strain vector, ϕ_δ, varies strongly in this parameter range, this being a direct consequence of the geometrical angular distortion of the complex; if the octahedron were regular, ϕ_δ would remain constant at 300°.

We consider the σ-donor capacity of oxygen ligators to be similar in magnitude to those of nitrogen ligators. Though it is true that nitrogen ligators lie further along oxygen ligators in the one-dimensional spectrochemical series, where the ligands are ordered according to their $3e_\sigma-4e_\pi$ values,[13] this is primarily a consequence of oxygen ligators being better π donors.[13] It is seen from Figure 2 that a strain vector in which the e_σ values for the oxygen-binding ligators are ∼7000 cm^{-1} bisects the cubic minima that correspond to elongated octahedra, in a direction that equates to a compression along the N2−Mn and Mn−O1 bond vectors, with $\delta = 1752$ cm^{-1} and $\phi_\delta = 55°$. In fact, varying the e_σ values of all ligands between 6500 and 7500 cm^{-1} always results in a strain vector that tends to stabilize a compression along these bond axes. It is reasonable to expect that the e_σ values of the ligands fall within this range. We conclude, therefore, that as a consequence of the combined effects of the pronounced geometrical angular distortion and the similar σ-donor capacities of the ligands, the low-symmetry strain calculated for complex **1** favors a compression along the N2−Mn and Mn−O1 bond vectors.

In order for a compression along the N2−Mn and Mn−O1 bonds to result, two criteria must be fulfilled. First, the tendency of the strain must be to locate the minimum at a point corresponding to a compression, i.e., $30° < \phi_\delta < 90°$, as is the case here; second, the strain must be large enough to counter the natural tendency of the molecule to form elongated octahedra, i.e., $\delta \gg 2\beta$. The second criterion is satisfied by choosing a value of A_2 that is moderate in magnitude. The joint effect of the cubic Jahn−Teller interaction and low-symmetry strain results in the potential energy surface shown in Figure 3. The surface consists of one minimum with the angular coordinate $\phi_\rho \approx \phi_\delta$.

Chloride is clearly a weaker σ donor than oxygen with e_σ toward the lower end of the values indicated in Figure 2. With the geometric constraints held constant, the effect of substituting oxygen for a weaker σ donor is a shift in the angular direction of the vector toward $\phi_\rho = 0°$ and a decrease in the magnitude, as documented in Table 2. It is then evident from Figure 2 that substituting the acetate and methoxide ligators by chloride favors an intramolecular reorientation, with the chloride complex adopting a tetragonally elongated octahedron with the long axis along the bond vectors labeled Mn−N1 and Mn−O2 in Figure 1.
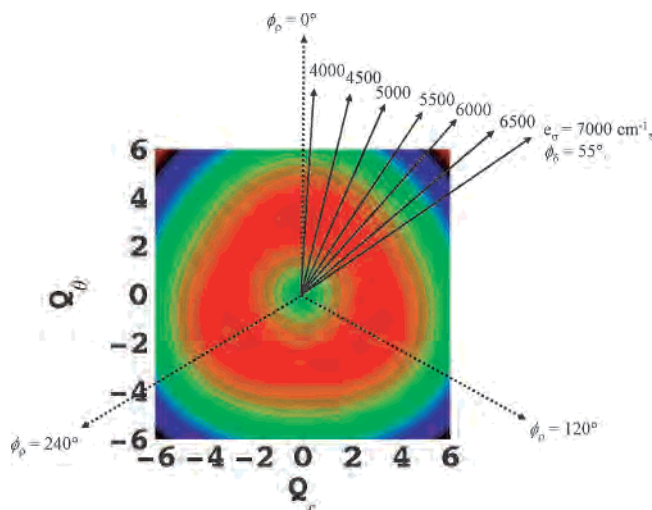
Figure 2. Cubic E⊗e Jahn−Teller potential energy surface calculated with the parameters $\hbar\omega = 450$ cm^{-1}, $A_1 = -1400$ cm^{-1}, and $A_2 = 10$ cm^{-1} in the $\{Q_\theta, Q_\epsilon\}$ coordinate frame. The barrier height is ∼193 cm^{-1} with the minima at angular positions of $\phi_\rho = 0°$, 120°, and 240°. Overlaid are vectors representative of the magnitude and angular direction of the strain interaction obtained from AOM calculations. The length of the arrows is proportional to δ, and the $\{e_\theta, e_\epsilon\}$ coordinate frame is co-incident with that of $\{Q_\theta, Q_\epsilon\}$ such that ϕ_δ varies from 3° to 55°. The AOM calculations (eqs 8 and 9) are for a complex based upon [Mn(bpia)(OAc)(OCH$_3$)]$^+$. The AOM angles are derived from the atomic positions of the complex and the e_σ values for the nitrogen ligators of the tripodal ligand fixed at 7000 cm^{-1}. The e_σ values for the remaining two ligators are varied between 4000 and 7000 cm^{-1}, as indicated in the figure. When δ is large compared with the barrier height ($2\beta \sim 2A_2(A_1/\hbar\omega)^2$), the potential energy minimum is dictated largely by the value of ϕ_δ.

In Table 2 are presented parameters pertaining to the strain vector, potential energy surface, ground-state wavefunction, and E/D values as a function of the e_σ values of the monodentate ligands. In the cubic approximation, in the limit where $\delta \gg 2\beta$, $|E|/D$ is determined largely by the value of ϕ_δ. The calculation shows that only when the e_σ values of the monodentate ligands are comparable to those of the tripodal ligand are the calculated values of $|E|/D$ in accordance with the value of 0.17 determined experimentally.[16] On substituting the acetate and methoxide ligands by chloride, a change in the sign of $|E|/D$ is predicted.

The conformational strain in **2** differs only slightly from that in **1** on account of the different ligand backbone and the results of our calculations for the two complexes are essentially the same. A more pronounced change in interligand steric repulsion is brought about by the substitution of the acetate and methoxide groups by chloride. Nevertheless, the dominant contribution to the geometrical distortion is the tripodal bpia/bipa ligand, and the internal angles of the atoms comprising the first coordination sphere change but marginally from complex to complex. Hence, when the calculation outlined above is repeated with the atomic positions of **3**, very similar results are obtained. A compression is predicted when the σ-bonding strength of the monodentate ligands is comparable to the tripodal ligand, permuting to an elongation along a different axis when the σ-bonding of the monodentate ligands are weaker in strength. The only difference being that the swing of the strain vector from the region 30° < ϕ_δ < 90° to the region −30° < ϕ_δ < 30° occurs more rapidly upon decreasing the e_σ values of
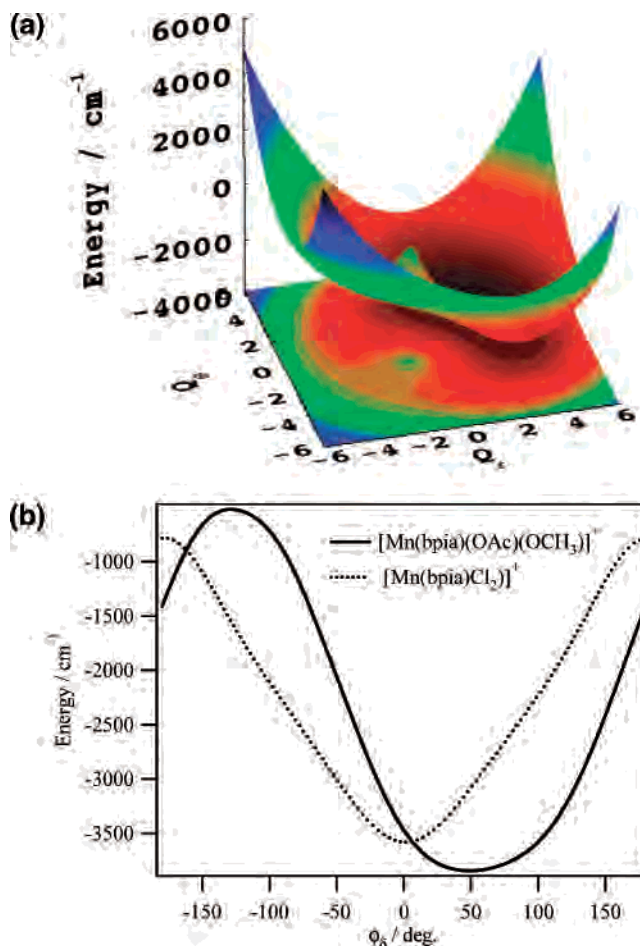
Figure 3. (a) E⊗e Jahn−Teller potential energy surface of a complex resembling [Mn(bpia)(OAc)(OCH$_3$)]$^+$. The parameters defining the cubic part of the Hamiltonian are $\hbar\omega = 450$ cm^{-1}, $A_1 = -1400$ cm^{-1}, and $A_2 = 10$ cm^{-1}. The low-symmetry crystal field was calculated using the AOM, as described in the text. The polar angles were generated from the atomic coordinates, and e_σ values of 7000 cm^{-1} were used to model the bonding interaction with both the nitrogen and oxygen ligators. (b) Display of the path of minimum energy as a function of the angular coordinate ϕ_δ. Also shown in b is the corresponding plot for the idealized [Mn(bpia)Cl$_2$]$^+$ complex, where the e_σ values for the monodentate ligands have been reduced to 4000 cm^{-1}, all other parameters remaining unchanged.

the monodentate ligands for complex **3** compared with complexes **1** and **2**.

One point needs to be emphasized concerning these calculations. The energy minimum on the E⊗e Jahn−Teller potential energy surface is a consequence of the competing effects of the low-symmetry strain and the warping of the surface, represented in this work by an effective second-order parameter, A_2. In the absence of relevant experimental data and electronic structure calculations, we have simply selected a value of this parameter to demonstrate the competing nature of the two interactions while ensuring that the dominant contribution is the strain. If the calculated strain is predicted to stabilize an elongation within the uncertainty of the geometric and bonding parameters, then an elongation along that axis is likely to occur. Conversely, if the calculated strain is predicted to stabilize a compression, then without a reasonable estimate of the A_2 parameter, one may state only that a compression is competitive.

Table 2. Effect of Ligand Substitution on the Structural and Electronic Properties of a Mn(III) Complex Resembling [Mn(bpia)(OAc)(OCH$_3$)]$^+$ ^{a}

e_σ	e_θ	e_ϵ	δ	ϕ_δ/deg	ϕ_{PE}/deg	ϕ_{vib}/deg	$|E|/D$
4000	1301	59	1302	3	1	1	−0.014
4500	1253	287	1285	13	7	7	−0.075
5000	1204	516	1310	23	13	14	−0.15
5500	1156	745	1375	33	19	19	−0.21
6000	1108	974	1474	41	27	31	0.29
6500	1060	1202	1603	49	37	41	0.20
7000	1011	1431	1752	55	49	51	0.10

^{a}This table reports vibronic coupling calculations in which the low-symmetry crystal field, calculated using eqs 6−9, is varied by changing the bonding strength of two ligands labeled O1 and O2 in Figure 1. The angular dispositions of the ligands are fixed at values calculated from the atomic coordinates of [Mn(bpia)(OAc)(OCH$_3$)]$^+$ (complex **1**). Following the labeling scheme of Figure 1, these are as follows N1, $\theta = 0°$, $\phi = 0°$; N5, $\theta = 74.5466°$, $\phi = 0°$; N2, $\theta = 79.2275°$, $\phi = 90.1145°$; N4, $\theta = 74.1201°$, $\phi = 179.532°$; O1, $\theta = 92.3365°$, $\phi = 271.627°$; O2, $\theta = 160.433°$, $\phi = 145.170°$. The e_σ values of the nitrogen ligands are fixed at 7000 cm^{-1}, and the e_σ values of ligands O(1) and O(2) vary according to the entries in column 1. It is anticipated that the values of e_σ pertaining to oxygen ligators fall at the upper end of these values while the values of e_σ pertaining to chloride ligators fall toward the lower end. Columns 2 and 3 are the strain parameters calculated by comparison of eqs 6 and 8. Converting these values to polar coordinates results in the entries given in columns 4 and 5. The column headed by ϕ_{PE} is the potential energy minimum calculated by diagonalization of eq 1 with $\hbar\omega = 450$ cm^{-1}, $A_1 = -1400$ cm^{-1}, and $A_2 = 10$ cm^{-1}. The last two columns correspond to the angular expectation value of the vibronic ground multiplet and the corresponding value of $|E|/D$, calculated by numerical diagonalization of the vibronic Hamiltonian.[3]

4. Summary and Conclusion

In this work, a simple formalism has been presented to predict the nature of the Jahn−Teller distortion in transition-metal complexes with orbital doublet ground terms. The method involves evaluating the low-symmetry component of the ligand field using the angular overlap model and considering how this strain perturbs a cubic E⊗*e* Jahn−Teller potential energy surface. The method has been successfully applied to rationalize the stereochemistries of a series of monomeric manganese(III) complexes formed with tetradentate tripodal ligands.

The massive angular distortion of the first coordination sphere imposed by the tetradentate tripodal ligands is predicted to give rise to a significant anisotropic strain that stabilizes a compression when the σ-donor strengths of the coordinating ligands are similar in magnitude. This condition is satisfied in compounds **1** and **2**, and it is indeed gratifying that the observed axes of compression are in accordance with the calculated strain vector. When the σ-donor strengths of the monodentate ligands are reduced, an elongation along a different axis is predicted, once again in accordance with the structure of compound **3**. The calculations aptly demonstrate how the plasticity of the coordination sphere is enhanced on account of the pronounced geometrical angular distortion.

Another series of manganese(III) compounds has been reported to exhibit similar structural properties.[14] The stereochemistry is again dominated by a polydentate ligand, and a compression or elongation is observed, depending on the identity of the monodentate ligands. Without providing details, we can state that the strain resulting from the angular distortion of the ligands alone leads to a value of ϕ_δ that is ~30° from the value that would stabilize the observed tetragonal compression and ~30° from the value that would stabilize the observed tetragonal elongation. A small swing of the strain vector resulting from the heteroleptic ligand field is needed for the compression to be competitive. Given these encouraging results, we believe that the method set out in this paper will be of use in predicting the nature of the Jahn−Teller distortion in bioinorganic manganese(III) and copper-(II) centers where the bond lengths cannot be accurately determined by protein crystallography but the angular geometry and σ-bonding capacity can be reasonably inferred from a knowledge of the coordinating ligands.